

# The effects of pH, temperature, and buffer concentration on the self-assembling behavior, secondary structure, and surface hydrophobicity of donkey and bovine $\beta$ -casein

Jingjing Zhang<sup>a,b,\*</sup>, Silvia Vincenzetti<sup>a</sup>, Paolo Polidori<sup>c</sup>, Valeria Polzonetti<sup>a</sup>, Alessandro Di Michele<sup>d</sup>, Diego Romano Perinelli<sup>c</sup>, Guiqin Liu<sup>b</sup>, Lanjie Li<sup>b</sup>, Stefania Pucciarelli<sup>a</sup>

<sup>a</sup> School of Biosciences and Veterinary Medicine, University of Camerino, Via Gentile III da Varano, 62032 Camerino, MC, Italy

<sup>b</sup> College of Agronomy, Shandong Engineering Technology Research Center for Efficient Breeding and Ecological Feeding of Black Donkey, Shandong Donkey Industry Technology Collaborative Innovation Center, Liaocheng University, 252000 Liaocheng, Shandong, China

<sup>c</sup> School of Pharmacy, University of Camerino, Via Gentile da Varano, 62032 Camerino, MC, Italy

<sup>d</sup> Department of Physics and Geology, University of Perugia, Via Alessandro Pascoli, 06123 Perugia, PG, Italy

## ARTICLE INFO

### Keywords:

Donkey  $\beta$ -casein  
Critical micelle concentration  
Critical micelle temperature  
Secondary structure  
Surface hydrophobicity

## ABSTRACT

The self-assembling behavior, secondary structure, and surface hydrophobicity of purified donkey  $\beta$ -casein in terms of pH, temperature, and buffer concentration were investigated in comparison with commercial bovine  $\beta$ -casein. Critical micelle concentration of both  $\beta$ -caseins decreased with the lowering of pH (pH 8.0–6.0) and the increasing temperatures (25–50 °C). Critical micelle temperature of both  $\beta$ -caseins increased moving from pH 6.0 to 8.0 and aggregates larger than micelles formed at pH 6.0 that is close to their isoelectric point. Fluorescence spectroscopy analysis demonstrated that the maximum surface hydrophobicity was achieved at pH 6.0. The secondary structure was examined using circular dichroism spectroscopy, highlighting an increase of  $\alpha$ -helix content and a decrease of unordered structures with the decrease of pH and increase of temperature. This work provides insights on parameters promoting molecular interactions involved in donkey  $\beta$ -CN self-association, useful to develop nanocarriers for encapsulating bioactive compounds in pharmaceutical and nutraceutical applications.

## 1. Introduction

Caseins represent the major fractions (50–80 %, w/w) of total milk proteins and have attracted much interest thanks to their peculiar structure and appealing functional properties (Tidona et al., 2014). The four caseins in milk that differ markedly in terms of structure and function are  $\alpha$ 1-caseins (~38 %),  $\alpha$ 2-caseins (~10 %),  $\beta$ -caseins (~34 %) and k-caseins (~15 %) (Ranadheera et al., 2016). In an aqueous environment, as in milk, they associate into supramolecular colloidal structures known as casein micelles, which are approximately spherical in shape with an average diameter of about 120 nm and a mass in the range of  $10^6$ – $10^9$  Da (Holt, 2013).

$\beta$ -casein ( $\beta$ -CN) is the major protein constituent, accounting for around 30 % of the total bovine caseins. Differently from the other

caseins,  $\beta$ -CN can self-assemble into a micellar structure under appropriate (e.g., physiological) conditions thanks to its amphiphilic structure, leading to the formation of energetically favored intermolecular hydrophobic interactions (Chia et al., 2017). Bovine  $\beta$ -CN consists of 224 amino acids and shows a molecular weight of ~24 kDa, and the secondary structure is widely represented by a random coil with considerable flexibility due to the lack of disulfide bonds (Raynes et al., 2015). The  $\beta$ -CN unique structural properties can depend on the presence of large amounts of proline residues, which strongly affect the protein structure due to their tendency to impair the formation of  $\alpha$ -helices and  $\beta$ -sheets and arrange in short segments of polyproline II-helices in a temperature-dependent behavior (Hasni et al., 2011). The formation of  $\beta$ -casein's self-assembled micelles in an aqueous environment is affected by many factors, the most important of which are protein concentration,

\* Corresponding author at: School of Bioscience and Veterinary Medicine, University of Camerino, Via Gentile III da Varano, 62032 Camerino, MC, Italy.

E-mail addresses: [jingjing.zhang@unicam.it](mailto:jingjing.zhang@unicam.it) (J. Zhang), [silvia.vincenzetti@unicam.it](mailto:silvia.vincenzetti@unicam.it) (S. Vincenzetti), [paolo.polidori@unicam.it](mailto:paolo.polidori@unicam.it) (P. Polidori), [valeria.polzonetti@unicam.it](mailto:valeria.polzonetti@unicam.it) (V. Polzonetti), [alessandro.dimichele@unipg.it](mailto:alessandro.dimichele@unipg.it) (A. Di Michele), [diego.perinelli@unicam.it](mailto:diego.perinelli@unicam.it) (D.R. Perinelli), [guiqinliu@lcu.edu.cn](mailto:guiqinliu@lcu.edu.cn) (G. Liu), [lilianjie@lcu.edu.cn](mailto:lilianjie@lcu.edu.cn) (L. Li), [stefania.pucciarelli@unicam.it](mailto:stefania.pucciarelli@unicam.it) (S. Pucciarelli).

<https://doi.org/10.1016/j.foodchem.2023.137285>

Received 4 February 2023; Received in revised form 23 August 2023; Accepted 24 August 2023

Available online 30 August 2023

0308-8146/© 2023 The Author(s). Published by Elsevier Ltd. This is an open access article under the CC BY-NC-ND license (<http://creativecommons.org/licenses/by-nc-nd/4.0/>).

ionic strength, pH, and temperature (Schulte et al., 2020). Specifically, the critical micelle concentration (CMC) of  $\beta$ -CN can range between 0.05 % and 0.2 % (w/v), while the critical micelle temperature (CMT) is normally above  $\sim 20^\circ\text{C}$  at a neutral pH (Perinelli et al., 2019; Portnaya et al., 2006). Therefore,  $\beta$ -CN exists mainly as monomers under CMC and CMT, while it starts to self-assemble through the formation of hydrophobic interactions as concentration and temperature increase, giving rise to micellar aggregates characterized by a hydrophobic core and a less dense hydrophilic outer layer (Dauphas et al., 2005).

The unique structural organization of  $\beta$ -CN micelles makes them suitable for encapsulation, stabilization, and protection of several hydrophobic bioactive molecules, such as polyphenols, fat-soluble vitamins, and oils (Forrest et al., 2005; Li et al., 2019). Recently, several studies have introduced  $\beta$ -CN micelles as natural potential nano vehicles for the entrapment and oral delivery of hydrophobic drugs as anticancer chemotherapeutics including mitoxantrone (MX) (Shapira et al., 2010).

In the literature, several studies have presented the chemical-physical characterization and applications of  $\beta$ -CN proteins, but all of them concern the protein of bovine origin. Indeed, structural information about donkey milk  $\beta$ -casein are very few and only regarding the primary structure. Donkey milk  $\beta$ -casein consists of a full-length form A (226 amino acids) and a spliced form named B (218 amino acids) characterized by the lack of the peptide  $_{27}\text{ESITHINK}_{34}$  in the exon 5. These two A and B forms are in turn phosphorylated carrying 5, 6 and 7 phosphate groups (Licitra, et al., 2019). Other authors described another  $\beta$ -casein variant characterized by higher molecular weight and the presence of 5, 6 and 7 phosphate groups (Chianese, et al., 2010).

The interest of the food industry in donkey milk is mainly due to its hypoallergenic properties; several authors have demonstrated that serum of patients affected by Cow's Milk Protein Allergy (CMPA) does not cross-react with caseins and whey proteins isolated by donkey milk (Monti et al., 2007; Vincenzetti et al., 2014).

Furthermore, in a previous work, it was demonstrated that donkey  $\beta$ -CN was not recognized by bovine anti- $\beta$ -CN antibodies and this could determine the low immunogenicity potential of the protein from donkey source (Perinelli et al., 2019). This may be due to that fact that the IgE and IgG allergenic epitopes of bovine  $\beta$ -CN found in CMPA patients lies in an amino acid sequence that is different in the donkey  $\beta$ -CN (Perinelli et al., 2019; Vincenzetti et al., 2022).

Considering the emerging interest of the food field in donkey milk, it is worth elucidating the self-assembling behavior of donkey  $\beta$ -CN in comparison to the protein of bovine origin with the aim to acquire basic knowledge to exploit donkey  $\beta$ -CN as a potential biomaterial for the encapsulation and delivery of active compounds and drugs. Specifically, this research focuses on the characterization of self-assembling properties and structural changes of purified  $\beta$ -CN (obtained from donkey milk) at different conditions of pH (from 5.5 to 9.0), temperature (from  $20^\circ\text{C}$  to  $50^\circ\text{C}$ ) and buffer concentration (50 mM and 250 mM) using fluorescence spectroscopy, dynamic light scattering, and far-UV circular dichroism. The obtained results were then compared to those from commercial bovine  $\beta$ -CN and analyzed under the same experimental conditions.

## 2. Materials and methods

### 2.1. Materials

The donkey milk used in this study (from animals at the mid-stage of lactation), was purchased from a local farm (Azienda Agricola Mamma Asina, Colmurano, MC), located in the Marche region and immediately stored at  $4^\circ\text{C}$ . The  $\beta$ -CN proteins of donkey's milk were obtained according to the method described below (section 2.2). Lyophilized bovine  $\beta$ -CN, used as reference, was purchased from Sigma Aldrich (St. Louis, MO).

Ultrapure water was produced using an Adrona Crystal EX Trace/HPLC/Bio water purification system (Adrona SIA, Riga, Latvia). The

reagent-grade chemicals used in this study were purchased from Sigma-Aldrich (St. Louis, MO).

### 2.2. Methods

#### 2.2.1. Purification of $\beta$ -CN from donkey milk

Native  $\beta$ -CN was extracted and purified from donkey milk as previously described (Perinelli et al., 2019) with some modifications. After separation from the whey proteins by isoelectric precipitation at pH 4.6, the donkey casein fraction (obtained from 10 mL of milk) was resuspended in 10 mL of buffer A (50 mM ammonium acetate, 8 M urea; pH 5.5) and subsequently subjected to cationic exchange chromatography by using Carboxymethyl cellulose (CM52, Whatman, Merck, Darmstadt, Germany). The column was equilibrated in buffer A (flow rate 0.5 mL/min) and eluted by a linear gradient between buffer A and buffer B (1 M ammonium acetate, 8 M urea; pH 5.5). The chromatographic peak corresponding to  $\beta$ -CN was identified by a 15 % SDS-PAGE followed by mass spectrometry analysis, performed as already described (Perinelli et al., 2019). More in detail, the electrophoresis was done as described by Laemmli (Laemmli, 1970), under reducing conditions using a 15 % acrylamide-bis acrylamide solution and the Mini Protean III apparatus (Bio-Rad, gel size  $7 \times 8 \text{ cm} \times 0.75 \text{ mm}$ ). Five micrograms of each sample were incubated with the denaturing loading solution (12 % glycerol; 1.2 % SDS; 5.4 %  $\beta$ -mercaptoethanol; saturated bromophenol blue) at  $100^\circ\text{C}$  for 5 min and then loaded onto the gel. Electrophoresis was performed with a constant voltage of 200 V. The proteins were visualized on the gel by Coomassie Blue staining (0.1 % Coomassie Brilliant Blue R250 in 50 % methanol and 10 % acetic acid). The relative purity of donkey's  $\beta$ -CN, respect to the total stained proteins has been assessed by densitometric analysis of the gel, using PDquest software (Version 7.1.1; Bio-Rad Laboratories). After electrophoresis, the protein band was subjected to the in-gel digestion procedure following the protocol of Shevchenko and co-workers (Shevchenko et al., 2006), and subsequently to the mass spectrometry analysis for protein identification performed as previously described (Vincenzetti et al., 2019).

The peak corresponding to  $\beta$ -CN was dialyzed against 50 mM and 20 mM phosphate buffer using dialysis membranes (Spectra/Por®, MWCO = 3000 Da, Spectrum Lab. Inc., Phoenix, AZ). After protein concentration determination (Bradford, 1976), the dialyzed  $\beta$ -CN was divided into 2.0 mg aliquots, dried by a Speed Vacuum concentrator (Savant SpeedVac™ Thermo Fischer Scientific, Waltham, MA, USA), and stored at  $-20^\circ\text{C}$  until use.

#### 2.2.2. Critical micelle concentration (CMC) determination by pyrene fluorescence emission

Steady-state fluorescence spectra of pyrene in the presence of various concentrations (from 0.0125 mg/mL to 5.0 mg/mL) of donkey and bovine milk  $\beta$ -CNs as a function of pH (6.0, 7.0, 8.0 and 9.0) and buffer concentrations (50 mM and 250 mM) were recorded at  $25^\circ\text{C}$  using a spectrofluorimeter (LS-55, PerkinElmer, equipped with a HAAKE C25 P thermostat). The fluorescence emission spectra (200–700 nm) were measured using an excitation wavelength  $\lambda_{\text{exc}} = 334 \text{ nm}$  and 5.0/3.0 nm slits. The ratio between the first (I) and third (III) vibronic bands' intensity of pyrene emission, respectively at 372 nm and 382 nm, was plotted against the  $\beta$ -CN concentration. The critical micelle concentration (CMC) of  $\beta$ -CNs was determined by fitting the experimental data using the following equation (GraphPad Prism 9.2; Equation 1):

$$Y = \frac{\text{Bottom} + (\text{Top} - \text{Bottom})}{1 + 10^{[(\text{LogCMC} - x) \cdot \text{Hillslope}]}} \quad (1)$$

where the Top and Bottom are two plateaus of the curve in the unit of Y axis, and the Hill slope is the steepness of the curve. Data were collected in triplicate.

The composition of the buffers was 50 and 250 mM phosphate buffer ( $\text{KH}_2\text{PO}_4/\text{Na}_2\text{HPO}_4$ ), pH 6.0; 50 and 250 mM Tris buffer (Tris/HCl), pH 7.0, 8.0, 9.0.

### 2.2.3. Critical micelle temperature (CMT) determination by dynamic light scattering (DLS)

$\beta$ -CN proteins from donkey and bovine milk were dissolved at the concentration of 5 mg/mL in the previously prepared buffers (50 mM and 250 mM) at various pH values (from 6.0 to 9.0) as for CMC determination. Then, protein solutions were analyzed in the range of temperature 10.0–40.0 °C with a stepwise increase of 2.5 °C using a Malvern Zetasizer NanoS (Malvern Instrument Worcestershire, UK), equipped with a backscattering detector at 173°. The mean average size of hydrodynamic diameter (according to volume % distribution) was recorded at the fixed position of 4.65 mm, after an equilibration time of 300 s for each measurement. Critical micelle temperature (CMT) values were determined by fitting the experimental data using sigmoidal model in Eq.2.

$$Y = \frac{\text{Bottom} + (\text{Top} - \text{Bottom})}{1 + \exp(\text{CMT} - x)/\text{slope}} \quad (2)$$

The van't Hoff enthalpy has been calculated from the best-fit parameters by the van't Hoff equation (Equation 3).

$$\frac{d \ln K_{\text{app}}}{dt} = \Delta H / RT^2 \quad (3)$$

in which R is the universal gas constant (8.314 J / mol·K), and the  $K_{\text{app}} = (Y - \text{Bottom}) / (\text{Top} - Y)$ .

### 2.2.4. Hydrophobicity determination by fluorescence spectroscopy

Fluorescence spectra of  $\beta$ -CN proteins from donkey and bovine milk at the concentration of 0.2 mg/mL were recorded using a spectrofluorimeter in a 1 cm quartz cell. The slit widths were set at 5/3.5 nm respectively in emission and excitation pathways. Each sample was measured in triplicate at various temperatures (from 20.0 to 50.0 °C), pH (from 6.0 to 9.0), and buffer concentrations (50 mM and 250 mM, respectively). Emission spectra were recorded between 300 and 450 nm with an excitation wavelength of 295 nm. The scan speed was set at 60 nm/min.

8-Anilino-1-naphthalene-sulfonate (ANS) binding to donkey and bovine  $\beta$ -CN at various temperatures (from 20.0 °C to 50.0 °C), pH (from 6.0 to 9.0) and buffer concentrations (50 mM and 250 mM, respectively) was assessed after 10 min incubation (in dark) of 0.2 mg/mL  $\beta$ -CN with different ANS concentration (from 0  $\mu$ M to 600  $\mu$ M). Fluorescence emission spectra were measured using excitation at 370 nm and bandwidths of 5.0/3.5 nm in excitation/emission channel. All measurements were done in triplicate. The hydrophobic parameters (expressed as hydrophobic surface and affinity index) were calculated according to this formula (Equation 4, adapted from (Möller & Denicola, 2002)):

$$F = F_{\text{max}} \left( \frac{K_a \cdot [\text{ANS}]^n}{n + K_a \cdot [\text{ANS}]^n} \right) \quad (4)$$

where F is the Fluorescence intensity,  $K_a$  is the affinity constant (corresponding to the affinity index), n is the binding sites (corresponding to the hydrophobic surface).

### 2.2.5. Circular dichroism (CD)

Far-UV CD spectra were recorded by Jasco J-810 Spectropolarimeter (Jasco Incorporated) in 0.2 cm-quartz cuvette Hellma 106-QS at donkey and bovine  $\beta$ -CN concentration of 0.3 mg/mL in 50 mM phosphate buffer. CD spectra were obtained at controlled temperature (from 10.0 to 40.0 °C) and pH (from 6.0 to 9.0). Each spectrum represents the average of three scans, acquired with a scan rate of 50 nm/min in the spectral range from 180 to 260 nm with a 1 nm data collection. Protein spectra were corrected by buffer subtraction and expressed as mean residue ellipticity (degrees  $\text{cm}^2/\text{dmol}$ ). For the estimation of protein secondary structure content data were processed using the software CONTIN (<https://dichroweb.cryst.bbk.ac.uk>) and compared with CD spectra measured from the basic set of proteins (Set 7) for which X-ray diffraction data are available (Whitmore & Wallace, 2008). Given the

high degree of unordered structure of  $\beta$ -caseins, the deconvolution of CD spectra obtained in this spectral region can only provide semi-quantitative estimation of the protein secondary structure's changes.

## 3. Results and discussion

### 3.1. Purification of $\beta$ -CN

The mass spectrometry analysis of the peak eluted from cation exchange chromatography gave as a result donkey  $\beta$ -CN (CASB\_EQUAS, Beta-casein *Equus asinus*, Mascot score 266, sequence: VMPFLKSPIVPFSEKQILNPTNGENLR). The purified donkey milk  $\beta$ -CN shows a purification grade of 92 % according to the densitometric analysis performed on the electrophoretic gel using the PDquest software (Version 7.1.1; Bio-Rad Laboratories) (Fig. SF1). The electrophoretic behaviour of donkey milk  $\beta$ -CN has been compared with that of a commercial bovine beta-casein (Sigma Aldrich, St. Louis, MO). The apparent higher molecular weight for both caseins (donkey and bovine) after the 15 % SDS-PAGE performed under reducing and denaturing conditions, has been described by several authors and could be due to a slower migration of caseins in SDS-PAGE because of the formation of a casein-SDS complexes that could influence the shape of the protein (Raak et al., 2018; Chakraborty and Basak, 2008). This effect could be enhanced if the electrophoresis is performed under reducing and denaturing condition (Sharma et al., 2021). In addition, the molecular weight of donkey  $\beta$ -CN of about 2 kDa higher than bovine one is justified by the extra 20 amino acids in its primary sequence (Perinelli et al., 2019).

### 3.2. Characterization of the self-assembling behavior of bovine and donkey $\beta$ -CNs

The amphiphilic properties of  $\beta$ -CNs are responsible for their self-assembling behavior into spheroidal micelles, which are strongly influenced by physicochemical factors such as pH, temperature and ionic strength (Zhou et al 2019). In order to assess the role played by these factors on the micellization phenomenon we have investigated their effect on CMC and CMT, which macroscopically define the behavior of self-assembling amphiphiles, including biopolymers. In the following sub-paragraphs the results obtained by pyrene fluorescence spectroscopy, and dynamic light scattering (DLS) are reported to investigate the effects of pH, temperature and buffer concentration on these parameters.

#### 3.2.1. Effect of pH, temperature, and buffer concentration on CMC of donkey and bovine $\beta$ -CN by pyrene fluorescence emission

Pyrene as a fluorescence extrinsic probe was used for the CMC determination of  $\beta$ -CN in this study. This method is based on the nonlinear relationship between protein concentration and the ratio of its fluorescence intensities at peaks I and III. The concentration corresponding to the sudden decrease of the curve (as determined from Eq. 1) is recognized as the CMC value, which is the minimum concentration at which micelles begin to form.

It is well-known that CMC values of bovine  $\beta$ -CN are drastically affected by a variety of factors that can change the hydration state of the protein, thereby favoring hydrophobic intermolecular interactions between protein monomers (Portnaya et al., 2006). To verify such effects also on the self-assembling of donkey  $\beta$ -CN, we performed experiments at different experimental conditions such as four different pH values (6.0, 7.0, 8.0 and 9.0), two different buffer concentrations (50 mM and 250 mM), and two different temperatures (25 and 50 °C). The obtained results were compared with those from bovine  $\beta$ -CN.

The changes of I/III pyrene fluorescence intensity ratio as a function of  $\beta$ -CN concentration (from 0.0125 mg/mL to 5 mg/mL) have been shown in Fig. SF2. All the obtained profiles have a sigmoidal shape (from pH 6 to 8) in which two plateau regions can be observed, indicating a similar self-assembling behavior as a function of protein concentration

for both  $\beta$ -CNs. The first plateau corresponds to the concentrations of protein when only monomers of  $\beta$ -CN are present in the solution, while the other one refers to the concentrations at which micelles have been formed. The intermediate region of the curve, instead, represents the range of concentrations in which the self-assembling transition occurs. CMC values at pH of 6.0–8.0 have been calculated from these profiles by fitting the experimental data with a sigmoidal model as shown in Table 1. On the contrary, the obtained profiles at pH 9.0 did not show a sigmoidal shape, making it impossible to calculate a CMC value by fitting these data at this pH, suggesting that no micellization occurs.

The CMC values for both donkey and bovine  $\beta$ -CNs showed an increasing trend within the investigated pH range (from pH 6.0 to 8.0) regardless of the buffer concentration and temperature. At 25 °C, the CMC value of donkey  $\beta$ -CN is around 0.30 mg/mL at pH 6.0, much lower than at pH 7.0 (~0.80 mg/mL) and pH 8.0 (~0.90 mg/mL). Similarly, the CMC value of bovine  $\beta$ -CN is around 0.45 mg/mL at pH 6.0, much lower than that at pH 7.0 (~0.90 mg/mL) and pH 8.0 (~1.20 mg/mL). At pH 9.0, the CMC values of both  $\beta$ -CN proteins cannot be determined. These results indicate that the self-assembly behavior of  $\beta$ -CN is strongly pH-dependent. In previous studies, the reported CMC values for bovine  $\beta$ -CN were usually in the range of 0.05–0.2 % (w/v) depending on different conditions (pH, temperature and concentration, etc.) (Portnaya et al., 2006), which are in agreement with those detected in our research (0.34 ~ 1.27 mg/mL). The CMC values of bovine  $\beta$ -CN proteins in the present study at pH 7.0, were slightly larger than those (~0.5 mg/mL) obtained by using DLS at pH 6.5 in 50 mM isotonic HEPES buffer (O'Connell et al., 2003), but nearly similar to those reported (~0.7 mg/mL) by using fluorescence spectroscopy in 100 mM isotonic phosphate buffer (Zhang et al., 2004). According to Perinelli et al. (2019), the CMC values of donkey  $\beta$ -CN and bovine  $\beta$ -CNs were 0.44 mg/mL and 0.57 mg/mL in 50 mM HEPES buffer (pH 7.3, 37 °C), respectively (Perinelli et al., 2019). The small differences in CMC values can be explained by the variability due to the buffer type and operating temperature. Overall, the changes in CMC in response to increasing pH can reflect the contribution of electrostatic interactions and hydrogen bonding in the micellization process: the decrease in amino acid protonation occurring at high pH might neutralize positively charged side chains, which could be engaged in salt bridges and/or hydrogen bonds established in the micellar structure. The increase of pH above the isoelectric point can gradually induce the denaturation of  $\beta$ -CN or neutralize its positively charged side chains, causing a more difficult self-association process for the protein (Qi et al., 2004). As regards the effect of temperature, the CMC values decreased with the temperature from 25 °C to 50 °C. Ellouze et al. (2021) found that the CMC of bovine  $\beta$ -CN decreased from around 0.5 wt% at 4 °C (pH 2.6) to 0.1 wt% at 24 °C, which was consistent with our study (Ellouze et al., 2021). The decrease in the CMC upon the raising temperature may be due to more hydrophobic groups being exposed at the higher temperature, which drives the formation of  $\beta$ -CN micelles at lower concentrations (Anema, 2021).

The effect of buffer concentration on CMC for both donkey and bovine  $\beta$ -CNs appears to be less pronounced than observed by pH changes. The CMC values of  $\beta$ -CN proteins were a little bit larger in 50 mM than in 250 mM buffer concentration, but no marked differences were observed, indicating a moderate impact of ionic strength on the self-assembling properties of both  $\beta$ -CN proteins, at these three pH values. Mikheeva et al. (2003) observed that Tris had less effect on the micellization behavior of  $\beta$ -CN, in comparison with other co-solutes including inorganic salts, urea, and ethanol, which was in close agreement with the results reported by our research (Mikheeva et al., 2003).

### 3.3. Effect of pH and buffer concentration on CMT of bovine and donkey $\beta$ -CNs by DLS

Critical micelle temperature (CMT), defined as the temperature at which proteins start to reversibly interact and form micelles, is another fundamental parameter to describe the self-assembly behavior of proteins with amphiphilic properties. In the present study, dynamic light scattering (DLS) was applied to investigate the changes in particle size distribution of both donkey and bovine  $\beta$ -CNs as a function of pH (from 6.0 to 9.0) and buffer concentrations (50 mM and 250 mM). The analyses were performed in the temperature range from 10 °C to 40 °C, in which CMT values are supposed to be found according to our previous investigation (Perinelli et al., 2019). Fig. 1. shows the average particle size values, expressed as hydrodynamic diameter, plotted versus temperature for donkey and bovine  $\beta$ -CN's solutions at different pH and buffer concentrations.

The measured particle size displayed a pH-dependent behavior over temperatures. At pH 7.0 and 8.0, all the obtained data have a sigmoidal trend in which two plateau regions can be observed, as occurs for a micellization process. The first one refers to the range of temperatures in which protein in the monomeric state is predominant. The second one, instead, indicates the range of temperature at which micelles populate and coexist with unimers. The middle region, since micellization is a dynamic process, represents an intermediate state in which unimers start to aggregate into micelles. From these plots, the CMT values were calculated and reported in Table 2.

With the increase in pH from 7.0 to 8.0, the CMT of donkey  $\beta$ -CN increased from 22.6 °C to 26.5 °C in 50 mM buffer, while that of bovine  $\beta$ -CN increased from 22.7 °C to 25.2 °C. In 250 mM buffer, the CMT of donkey  $\beta$ -CN increased from 25.68 °C to 28.99 °C, while that of bovine  $\beta$ -CN increased from 21.6 °C to 23.1 °C. As a result, the CMT values of donkey and bovine  $\beta$ -CN do not have marked differences as a function of buffer concentration. In fact, micelles can form at pH 7.0 and pH 8.0 for both  $\beta$ -CNs. Compared to pH 8.0, the inflection point (CMT) of the curve at pH 7.0 appears at a lower temperature, indicating that micellization is favored at this pH for both  $\beta$ -CNs. The hydrodynamic diameter of protein monomers are of about 8–14 nm, while the micelles have a measured diameter of around 24–30 nm. Such values are in agreement with those

**Table 1**

Critical micelle concentration (CMC) values calculated by spectrofluorimetry using pyrene as fluorescent probe as a function of pH (6.0, 7.0, 8.0, and 9.0), temperature (25 and 50 °C) and buffer concentrations (50 mM, 250 mM, respectively). Number of repeats, n = 3.

CMC (mg/mL) determination (pyrene fluorescence)									
		25 °C				50 °C			
		50 mM buffer		250 mM buffer		50 mM buffer		250 mM buffer	
		mg/mL	R <sup>2</sup>	mg/mL	R <sup>2</sup>	mg/mL	R <sup>2</sup>	mg/mL	R <sup>2</sup>
<b>Donkey</b>	pH 6.0	0.32 ± 0.04	0.97 ± 0.00	0.31 ± 0.01	0.80 ± 0.00	0.27 ± 0.01	0.96 ± 0.00	0.24 ± 0.01	0.97 ± 0.00
	pH 7.0	0.74 ± 0.01	0.99 ± 0.00	0.80 ± 0.18	0.82 ± 0.01	0.66 ± 0.03	0.98 ± 0.00	0.63 ± 0.01	0.98 ± 0.00
	pH 8.0	0.94 ± 0.04	0.91 ± 0.01	0.91 ± 0.10	0.95 ± 0.00	0.84 ± 0.01	0.98 ± 0.00	0.81 ± 0.01	0.98 ± 0.01
	pH 9.0	n.d.	–	n.d.	–	n.d.	–	n.d.	–
<b>Bovine</b>	pH 6.0	0.51 ± 0.01	0.99 ± 0.00	0.43 ± 0.14	0.93 ± 0.01	0.42 ± 0.01	0.98 ± 0.00	0.34 ± 0.01	0.99 ± 0.00
	pH 7.0	0.91 ± 0.03	0.97 ± 0.00	0.96 ± 0.09	0.71 ± 0.02	0.73 ± 0.01	0.94 ± 0.00	0.70 ± 0.00	0.96 ± 0.00
	pH 8.0	1.27 ± 0.05	0.98 ± 0.01	1.15 ± 0.26	0.78 ± 0.01	1.10 ± 0.00	0.94 ± 0.01	0.97 ± 0.01	0.96 ± 0.00
	pH 9.0	n.d.	–	n.d.	–	n.d.	–	n.d.	–



## Donkey

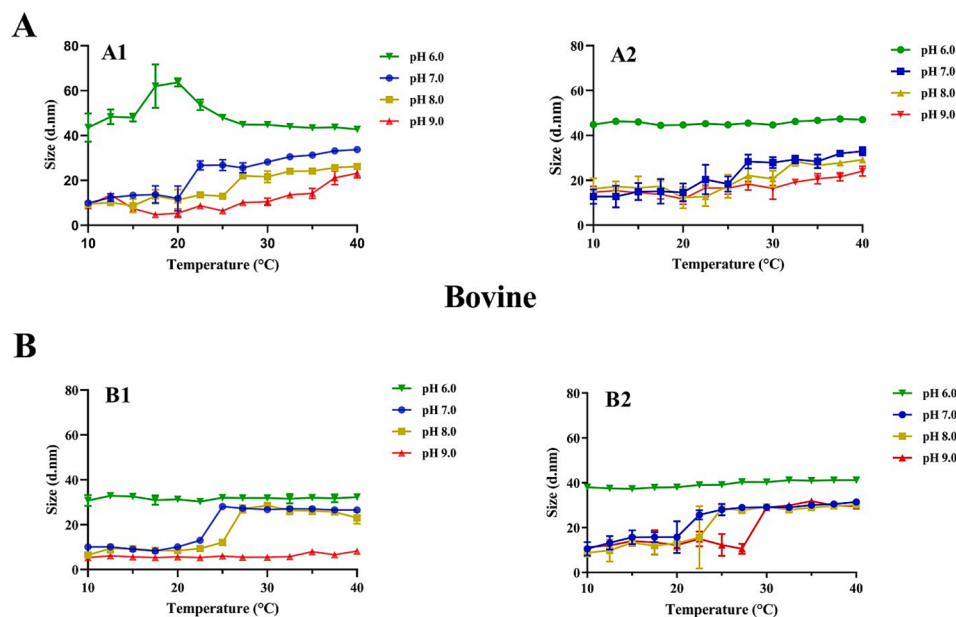


**Fig. 1.** Variation of the hydrodynamic diameter (nm) over temperature for donkey and bovine  $\beta$ -CN as a function of pH value (6.0, 7.0, 8.0, and 9.0) at concentration of 5 mg/mL, buffer concentration is 50 mM (A1) and (B1), buffer concentration is 250 mM (A2) and (B2).

**Table 2**

Critical micelle temperature (CMT) values calculated by dynamic light scattering (DLS) as a function of pH at room temperature in different buffer concentrations (50 mM, 250 mM, respectively). Number of repeats,  $n = 3$ .

CMT (°C) determination (DLS)									
Donkey	50 mM buffer		250 mM buffer		Bovine	50 mM buffer		250 mM buffer	
	°C	R <sup>2</sup>	°C	R <sup>2</sup>		°C	R <sup>2</sup>	°C	R <sup>2</sup>
pH 6.0	n.d.	–	n.d.	–	n.d.	–	n.d.	–	–
pH 7.0	22.6 ± 1.5	0.89 ± 0.00	25.7 ± 1.5	0.81 ± 0.00	22.7 ± 0.53	0.99 ± 0.00	21.6 ± 1.7	0.81 ± 0.01	–
pH 8.0	26.5 ± 1.2	0.89 ± 0.00	29.0 ± 5.7	0.81 ± 0.01	25.2 ± 0.59	0.96 ± 0.00	23.1 ± 3.5	0.81 ± 0.01	–
pH 9.0	n.d.	–	n.d.	–	n.d.	–	n.d.	–	–

from previous studies (Perinelli et al., 2019). Perinelli et al. (2019) found that the hydrodynamic diameter of  $\beta$ -CN as monomers was in the range of 6–10 nm and around 26–27 nm for the micellar aggregates (Perinelli et al., 2019). More recently, Wu et al. (2021) reported that the particle size distribution of buffalo  $\beta$ -CN monomer was about 10 nm, and protein gradually aggregated with the decrease in pH values (Wu et al., 2021). The pH effect on CMT of the protein was explained by altering the ionization of protein functional groups and double-layer thickness to lead to more exposure of hydrophobic groups (Boulet et al., 2001).

On the contrary, both donkey and bovine  $\beta$ -CNs are more aggregated at pH 6.0 with a particle size of  $\sim 40$  nm, larger than that measured for micelles. This marked increase in size can be explained by taking into account that pH 6.0 is closer to the isoelectric point of  $\beta$ -CN (around pH 5.2) (Wüstneck et al., 2012). The formation of these aggregates can be driven by the tendency of the protein to reduce its electrical charge, thereby affecting solubility.

Despite the very similar CMT values observed for donkey and bovine  $\beta$ -CNs at all the explored pH, the slope of temperature responsiveness varied substantially between the two proteins. According to van't Hoff equation (2) the slope of temperature induced transition is proportional to the difference in enthalpy between the unimeric and micellar states. By the sigmoidal fit of the data shown in Fig. 1, we have calculated the van't Hoff enthalpy of micellization at pH 7 and 8 (buffer concentration

250 mM) for both  $\beta$ -CNs. The results were  $21.25 \pm 7.84$  kJ/mol at pH 7, and approximately 49.62 kJ/mol at pH 8 for bovine  $\beta$ -CN, while  $8.27 \pm 3.1$  kJ/mol at pH 7 and  $9.13 \pm 4.6$  kJ/mol at pH 8 for donkey  $\beta$ -CN, values remarkably lower than the ones observed for the bovine protein. This difference was even more evident at the buffer concentration 50 mM (data not shown).

Increasing the pH up to 9.0 had a negative effect on the micellization process of both  $\beta$ -CNs. This resulted in a non-complete micellization process, in most cases, in the range of the experimental temperatures (10–40 °C). This behavior could be related to the deprotonation of some basic amino acids, involved in hydrogen bonding. Therefore, the micellar structure of both  $\beta$ -CNs seems to be destabilized by alkaline pH and require a higher temperature to form, and eventually relax at pH 9.0, as reported elsewhere (Ellouze et al., 2021).

Noticeably, the CMT and the van't Hoff enthalpy of micellization values of bovine  $\beta$ -CN obtained by DLS in this study were comparable to those calculated from other techniques, such as high-sensitivity differential scanning calorimetry and isothermal titration calorimetry (Mikheeva et al., 2003; Portnaya et al., 2006).

### 3.4. Characterization of the hydrophobic properties dependence on pH, temperature and buffer concentration of bovine and donkey $\beta$ -CNs

Hydrophobic effect is one of the most important non-covalent interactions involved in micelles self-assembling.  $\beta$ -caseins amphiphilic properties rely on an N-terminal polar region and an apolar C-terminal tail (residues 136–209) that drives the micelle formation by hydrophobic effect. A tryptophan residue is present in the  $\beta$ -CNs hydrophobic region allowing the measurement of intrinsic Trp fluorescence

measurements to explore conformational modifications involving the hydrophobic tail, and that can affect micelle formation. In addition, being intrinsically disordered proteins (IDP),  $\beta$ -CNs present an extended structure offering a wide binding surface area available for ligands, which can be used as extrinsic fluorescent probes, such as ANS. All the experiments reported below have been performed at a concentration lower than CMC; this choice has been determined not only by technical reasons but also to investigate the effect of pH, temperature and ionic strength on the structural properties of the unimeric  $\beta$ -CNs leading to the

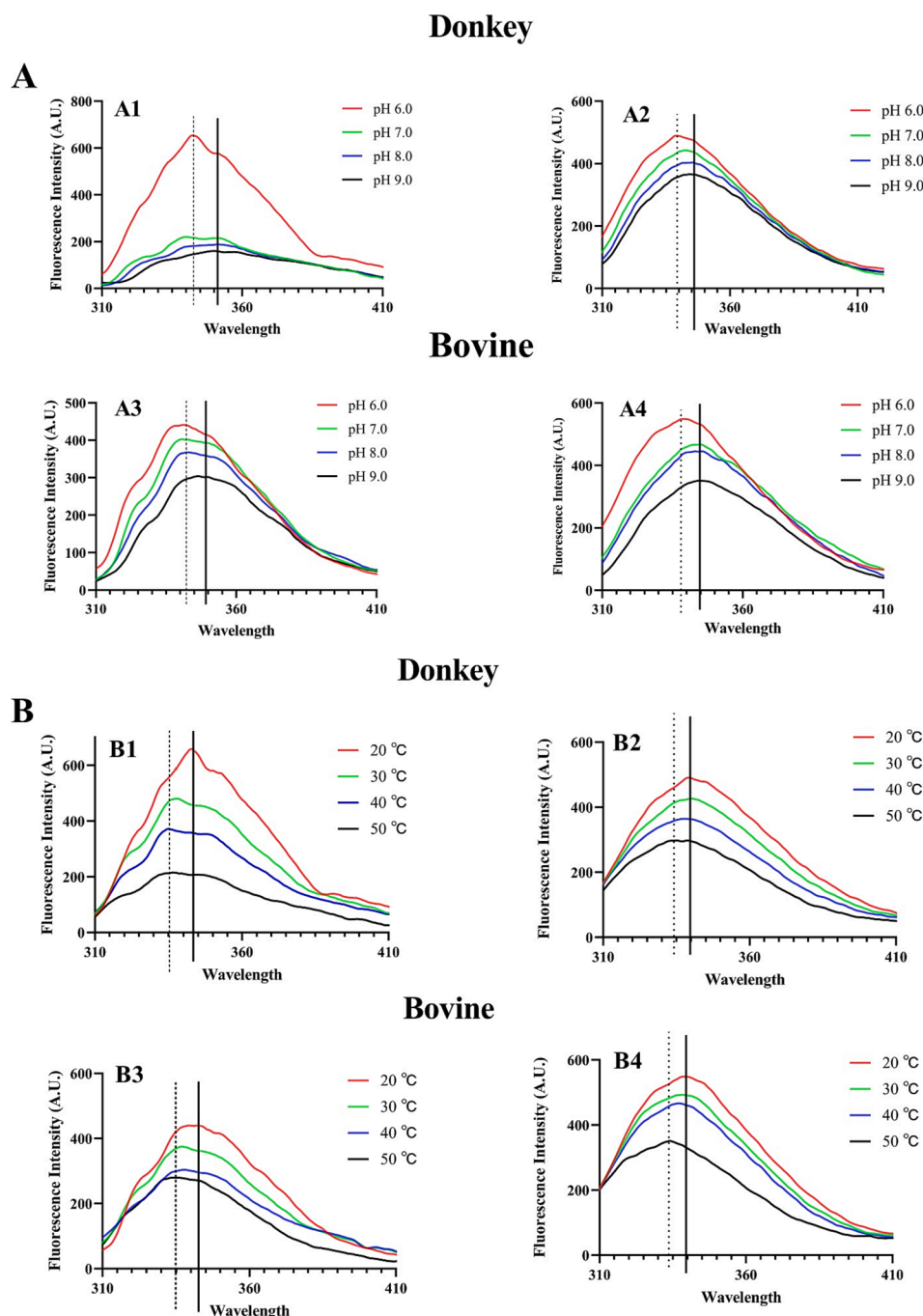


**Fig. 2.** (A) Tryptophan intrinsic fluorescence spectra of  $\beta$ -casein from donkey and bovine as a function of pH value (6.0, 7.0, 8.0, and 9.0) at concentration of 0.2 mg/mL (lower than CMC); buffer concentration is 50 mM (A1) and (A3), and 250 mM (A2) and (A4). The dotted line represents maximum fluorescence at around 340 nm at pH 6.0 and the solid line represents maximum fluorescence at around 350 nm at pH 9.0. (B) Tryptophan intrinsic fluorescence spectra of  $\beta$ -casein from donkey and bovine as a function of temperature (20 °C, 30 °C, 40 °C, and 50 °C) at concentration of 0.2 mg/mL (lower than CMC); buffer concentration is 50 mM (B1) and (B3), and 250 mM (B2) and (B4). The dotted line represents maximum fluorescence at around 335 nm at temperature 50 °C and the solid line represents maximum fluorescence at around 340 nm at temperature 20 °C.

micellization phenomenon.

### 3.4.1. Hydrophobic properties of $\beta$ -CNs examined by Trp fluorescence spectroscopy

The single Trp143 residue located in the hydrophobic domain of bovine  $\beta$ -CN primary structure has a high absorption and fluorescence yield, which can be used as an intrinsic fluorescent probe to study the protein's hydrophobic properties (Moeiniafshari et al., 2015). Moreover, the fluorescence intensity of tryptophan fluorophore was strongly influenced by its microenvironment. In the present study, the intrinsic Trp fluorescence of donkey and bovine  $\beta$ -CNs was measured to evaluate their structural changes induced by changes of pH (from 6.0 to 9.0), temperature (from 20 °C to 50 °C) and buffer concentrations (50 mM and 250 mM), respectively. The presence of a tryptophan residue in the  $\beta$ -CN from donkey milk has been confirmed by a search carried out in a protein database (<https://www.expasy.org/resources/uniprotkb-swiss-prot>) where it is possible to find an isoform of this protein showing a tryptophan residue in the third position of the amino acid sequence (accession number: A0A8C4ME87 · A0A8C4ME87\_EQUAS). Fig. 2A shows the changes in the relative fluorescence intensity of donkey and bovine  $\beta$ -CN at various pH values. As the pH decreased from 9.0 to 6.0, a gradual increase in the fluorescence intensity coupled with a blue shift to its maximum fluorescence (from  $\sim$  350 to  $\sim$  340 nm) was observed, reflecting the transfer of Trp to a more apolar environment. The temperature effect of both  $\beta$ -CN proteins on the Trp fluorescence intensity was presented in Fig. 2B.

It was interesting to find out that, the fluorescence intensity was decreased accompanied by a blue shift to its maximum fluorescence (from  $\sim$  342 to  $\sim$  333 nm) when temperature shifted from 20 °C to 50 °C. The fluorescence blue shift can be interpreted as a change in Trp environment's polarity, due to the self-association of  $\beta$ -CN via hydrophobic interactions, burying Trp residues from water molecules. These results are in agreement with Yousefi's et al (2009) research, which reported that the polarity of Trp environment of bovine  $\beta$ -CN undergoes a change in polarity and its emission intensity decreases by increasing temperature (Yousefi et al., 2009). The main reason for this phenomenon is the quenching of protein fluorescence intensity at high temperatures, showing a temperature-induced compaction of  $\beta$ -CN structure. In addition, a change in the geometry of  $\beta$ -CNs micelle induced by temperature could decrease its compaction as previously studied (O'Connell et al., 2003).

Furthermore, the buffer concentration has a greater effect on the fluorescence intensity of donkey  $\beta$ -CN than that of bovine (Fig. 2A and B); focusing on donkey  $\beta$ -CN under the same pH condition, the fluorescence intensity at a high buffer concentration (250 mM) was significantly higher compared with that measured at a low concentration (50 mM).

Therefore, the low pH, high temperature, and high buffer concentration appear to induce a structural change of both  $\beta$ -CN from donkey and bovine milk resulting in the hydrophobic tail intra- or intermolecular self-association protecting the tryptophan residues from the aqueous environment and promoting the more favorable micelle formation (Yousefi et al., 2009).

Wu et al. (2021) have found that the Trp fluorescence of  $\beta$ -CN was enhanced with a blue shift to its maximum value over the decrease in pH (from 7.5 to 5.0) and the increase in NaCl concentration (from 0.01 M to 0.30 M), which is consistent with our research (Wu et al., 2021).

### 3.4.2. Hydrophobic properties of $\beta$ -CNs examined by 8-anilino-1-naphthalene-sulfonic acid (ANS) binding fluorescence analysis

The use of ANS as an anionic fluorescent probe is one of the most common methods for the determination of protein hydrophobicity. Such a method is based on the binding of ANS with hydrophobic (nonpolar) surfaces of proteins, resulting in increased fluorescence intensity and a blue shift of its fluorescence maximum (Helmick et al., 2023). To further explore the hydrophobicity of  $\beta$ -CN, the binding of ANS was monitored

at concentrations ranging from 10  $\mu$ M to 600  $\mu$ M, as a function of pH (from 6.0 to 9.0), temperature (from 20.0 °C to 50.0 °C) and buffer concentration (50 mM and 250 mM), respectively. Fig. SF3 and Fig. SF4 showed that the studied  $\beta$ -CN proteins had different abilities to enhance ANS fluorescence intensity. The formula in Equation 4 can be used to determine the number of ANS binding sites ( $n$ ) per protein molecule and the dissociation constant ( $K_d$ ). After fitting the data, the influence of pH on the surface hydrophobic parameters ( $n$ ,  $K_a$  and  $K_d$ ) of  $\beta$ -CN proteins were summarized in Table ST1. The results indicated that both  $\beta$ -CN proteins had a high number of binding sites ( $n \geq 1$ ) with low affinity at pH 6.0. As the pH values increased from 6.0 to 9.0, an increase in the number of hydrophobic binding sites (protein-bound ANS) and a decrease in the affinity constant were observed. Furthermore, the relative fluorescence intensity of ANS bound to  $\beta$ -CN decreased and the fluorescence maximum had a red shift from pH 6.0 to pH 9.0 (Fig. SF5).

In particular, as reported in Table ST1, we could observe a higher affinity for ANS to donkey  $\beta$ -CN at 20 °C in the entire pH range 6-9, and that high alkaline pH caused the reduction of the number of the hydrophobic binding sites for ANS, with increased affinity, on both  $\beta$ -CNs. The titration of protein solutions with increasing concentrations of the fluorescent probe (ANS) can provide information on the surface hydrophobicity and affinity index of binding sites as a function of pH (Fig. 3A) (Annan et al., 2006).

In Table ST2, the calculated surface hydrophobic parameters ( $n$ ,  $K_a$ , and  $K_d$ ) of two  $\beta$ -CN proteins at pH 6.0 in terms of temperature effect (from 20 °C to 50 °C) were reported. These data indicated that both donkey and bovine  $\beta$ -CNs had a low number of binding sites ( $n \leq 1$ ) with high affinity at low temperature of 20 °C. Generally, with the increase in temperature from 20 °C to 50 °C, the number of binding sites of protein for ANS was increased and their affinity was gradually reduced (Fig. 3B). Meanwhile, with increasing temperature, there was a blueshift of the fluorescence maximum value. However, a gradual decrease in the relative fluorescence intensity was observed (Fig. SF6), suggesting that the fluorescence quenching has occurred, which was the same phenomenon as the intrinsic Trp fluorescence described before. Changes in surface hydrophobicity of  $\beta$ -CN confirmed that the heating process loosens the protein structure, and then more hydrophobic binding sites were exposed to the solvent. This can explain the temperature-induced and concentration-dependent micellization process of  $\beta$ -CN. O'Connell et al. (2003) reported the number of surface or accessible hydrophobic sites in  $\beta$ -CN progressively increased with the increasing temperature, in agreement with our results (O'Connell et al., 2003).

It should also be mentioned that the buffer concentration effect on the hydrophobic surface exposure of donkey  $\beta$ -CN was slightly more pronounced than in bovine protein. At each pH or temperature, the number of hydrophobic binding sites of donkey  $\beta$ -CN in 250 mM buffer was significantly higher than that in 50 mM buffer, while there was no evident difference in the hydrophobic surface exposure of bovine  $\beta$ -CN as a function of the two buffer concentrations. This may be due to the small differences in the amino acid sequence between donkey  $\beta$ -CN and bovine  $\beta$ -CN. In addition, the result was consistent with our previous description using Trp as the intrinsic fluorescent probe.

Thus, it can be seen that the fluorescence intensity of both donkey and bovine  $\beta$ -CNs bound to ANS was influenced by pH, temperature, and buffer concentration. The increase in surface hydrophobicity of  $\beta$ -CN suggested that a rearrangement of its structure led to the larger exposure of hydrophobic regions, especially at a lower pH (pH 6.0), a higher temperature (50 °C) and a higher buffer concentration (250 mM).

### 3.5. Analysis of secondary structure of $\beta$ -CNs by far-UV circular dichroism (CD)

The self-assembly phenomenon involved in  $\beta$ -CN micellization is thermodynamically controlled by supramolecular interactions, according to three-dimensional constraints that are encoded in the structural motifs of individual proteins (Mendes et al. 2013). Circular dichroism

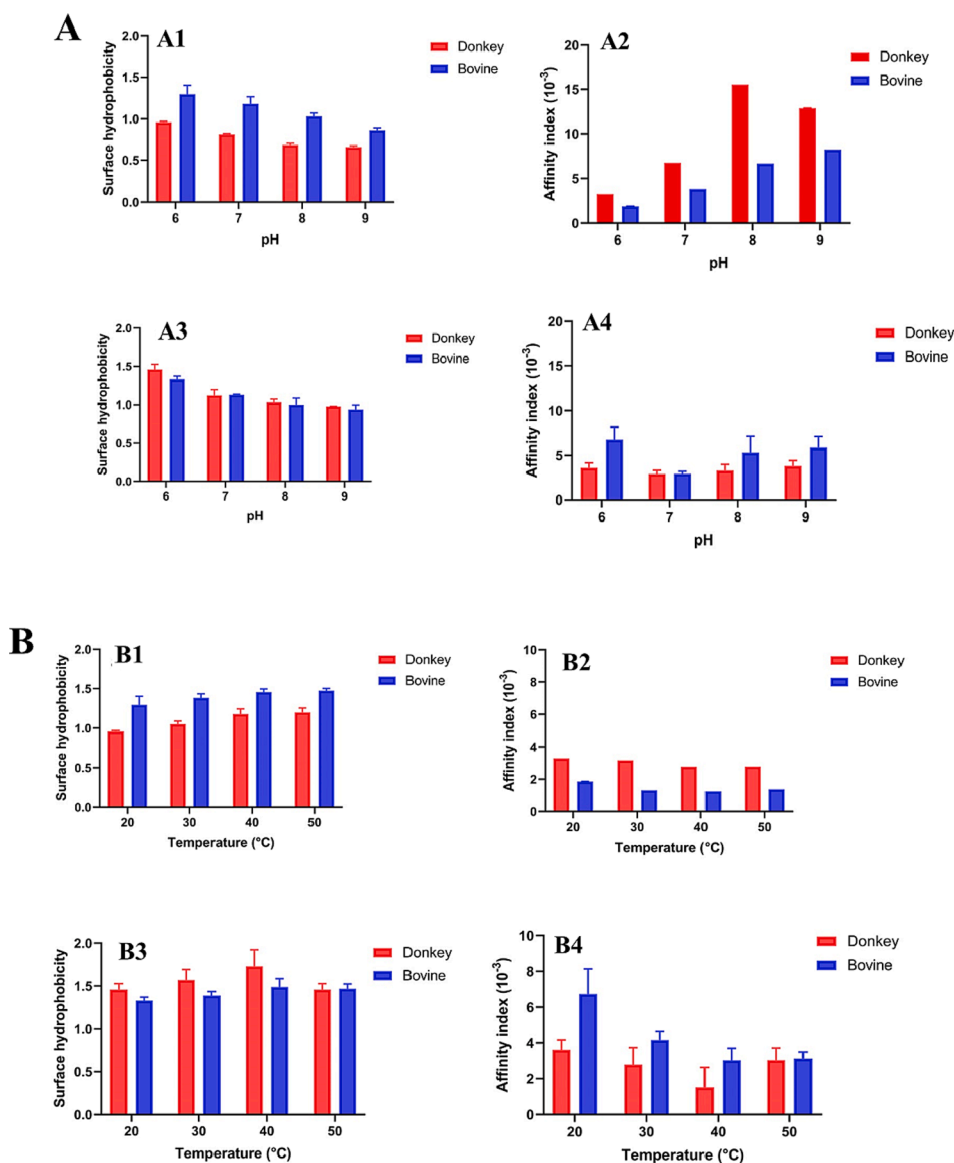


**Fig. 3.** (A) Hydrophobicity variation of donkey and bovine  $\beta$ -CNs as a function of pH value (6.0, 7.0, 8.0, and 9.0), surface hydrophobicity index in 50 mM buffer concentration (A1), affinity index in 50 mM buffer concentration (A2), surface hydrophobicity index in 250 mM buffer concentration (A3), affinity index in 250 mM buffer concentration (A4). (B) Hydrophobicity variation of donkey and bovine  $\beta$ -CNs as a function of temperature (20 °C, 30 °C, 40 °C, and 50 °C), surface hydrophobicity index in 50 mM buffer concentration, pH 6 (B1), affinity index in 50 mM buffer concentration, pH 6 (B2), surface hydrophobicity index in 250 mM buffer concentration, pH 6 (B3), affinity index in 250 mM buffer concentration, pH 6 (B4).

can thus provide helpful information in the secondary structure involvement in the micellar organization.

The conformational changes of the secondary structure in donkey and bovine  $\beta$ -CN in terms of different pH and temperature were detected by monitoring the alterations in the far-UV CD spectra (Fig. 4A and Fig. 4B).

The CD spectra of both donkey and bovine  $\beta$ -CNs at various pH values (pH 6.0, 7.0, 8.0, and 9.0) in 50 mM phosphate buffer at temperatures of 10.0 °C, 20.0 °C, 30.0 °C, and 40.0 °C, are shown in Fig. 4A. With the decreasing pH values from 9.0 to 6.0, there was a slight shift of the wavelength from about 198 to 202 nm with an increase in the negative value of ellipticity at the observed  $\lambda_{\text{max}}$  ( $\theta_{\text{R}}-200$  nm). Meanwhile, the negative peak intensity between the shoulders in the region between 215 and 230 nm was decreased. The obtained CD spectra changes of  $\beta$ -CN from both donkey and bovine as a function of pH values were close to those previously reported (Wu et al., 2021). CD spectra of both donkey and bovine  $\beta$ -CNs recorded at different pH values did not display isodichroic points, showing a monotonic change in the secondary structure (Faizullin et al., 2017).

Fig. 4B shows the temperature dependence of CD spectra of both donkey and bovine  $\beta$ -CNs at all detected pH values. All these spectra have a minimum ellipticity around 200 nm and a secondary negative

trough between 210 and 230 nm, which has been observed by Farrell et al. (2001) in the case of native  $\beta$ -CN (Farrell et al., 2001). With the increase in temperature from 10.0 °C to 40.0 °C,

the maximum negative CD peak at 200 nm was reduced along with a small shift of the negative peak from about 198 to 202 nm in both donkey and bovine  $\beta$ -CNs. Meanwhile, the negative peak between the shoulders of 215–230 nm gradually increased.

Taking into account that the optical activity observed in the region between 215 and 230 nm is dominated by electronic transitions  $n > \pi^*$  of the non-bonding carboxylic oxygen in the polypeptide backbone, it suggested that the  $\alpha$ -helix content was increased with the increasing temperature. This behavior is quite different from that of a typical globular protein that displays temperature-induced reduction of  $\alpha$ -helical content, and it may be due to an increase in polyproline II helix structure and self-association beginning to take place with increased temperature, as noted above (Qi et al., 2004; Kuemin et al., 2010). Gangnard et al. (2007) also demonstrated that the CD spectra showed an upward shift of ellipticity at 200 nm and a downward shift in the 210–230 nm with the increasing temperature, as observed in our study (Gangnard et al., 2007).

The composition of  $\beta$ -CN secondary structure of donkey and bovine is given in Table ST3, and we found that there was little change in the



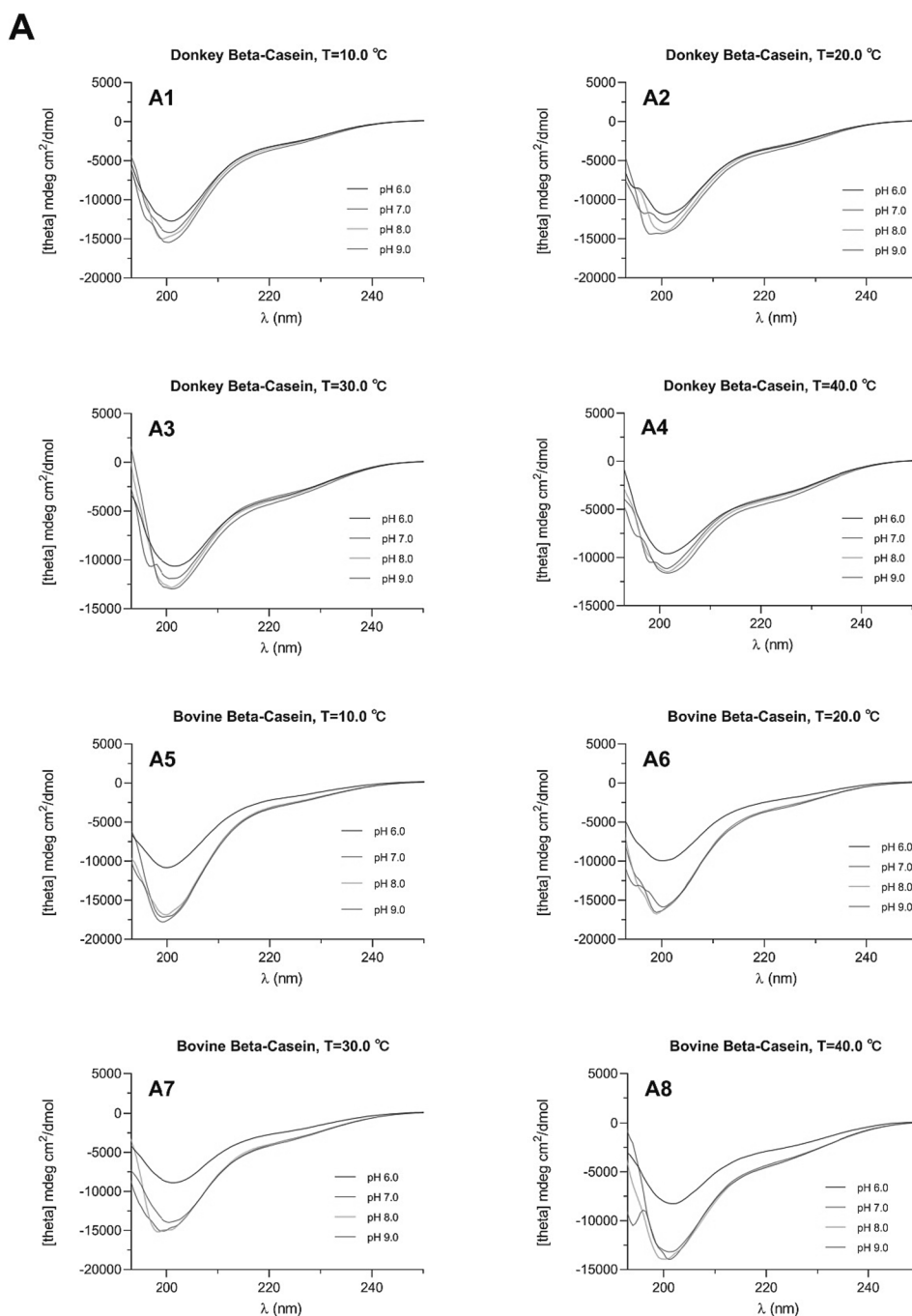


**Fig. 4.** (A) Circular dichroism spectra of donkey  $\beta$ -CN (0.3 mg/mL) as a function of pH value (6.0, 7.0, 8.0, and 9.0) at 10.0 °C (A1), 20.0 °C (A2), 30.0 °C (A3), 40.0 °C (A4); Circular dichroism spectra of bovine  $\beta$ -CN (0.3 mg/mL) as a function of pH value (6.0, 7.0, 8.0, and 9.0) at 10 °C (A5); 20 °C (A6); 30 °C (A7); 40 °C (A8). (B) Circular dichroism spectra of donkey  $\beta$ -CN (0.3 mg/mL) as a function of temperature (10 °C, 20 °C, 30 °C, 40 °C) at pH 6.0 (B1), 7.0 (B2), 8.0 (B3), 9.0 (B4); Circular dichroism spectra of bovine  $\beta$ -CN (0.3 mg/mL) as a function of temperature (10.4 °C, 20 °C, 29.6 °C, 40 °C) at pH 6.0 (B5), 7.0 (B6), 8.0 (B7), 9.0 (B8);

calculated amounts of unordered, helix, turns, or sheet structure. Generally, the content of  $\alpha$ -helix was increased and the unordered structure was decreased at pH values from 9.0 to 6.0 at all temperatures. With the increase in the temperature from 10.0 °C to 40.0 °C, at all pH values, the composition in  $\alpha$ -helix increased, while unordered structure decreased. However, compared with  $\alpha$ -helix and unordered structure, the composition in  $\beta$ -strands and turns did not display significant changes in terms of pH and temperature. Faizullin et al (2017) reported that at 10 °C in the buffer solution,  $\beta$ -CN possesses 10 % of helical, 12 % extended, 14 % turns, and 64 % unordered structural content, in close

agreement with our results on secondary structure of donkey and bovine  $\beta$ -CNs (Faizullin et al., 2017).

#### 4. Conclusions

Analogous self-assembling behavior as a function of protein concentration, temperature, and pH was found for donkey and bovine  $\beta$ -CNs. pH exerted a strong effect on both CMC and CMT, suggesting a strong contribution of electrostatic interactions and hydrogen bonding in the micellization process. Micelles formation of both  $\beta$ -CNs was

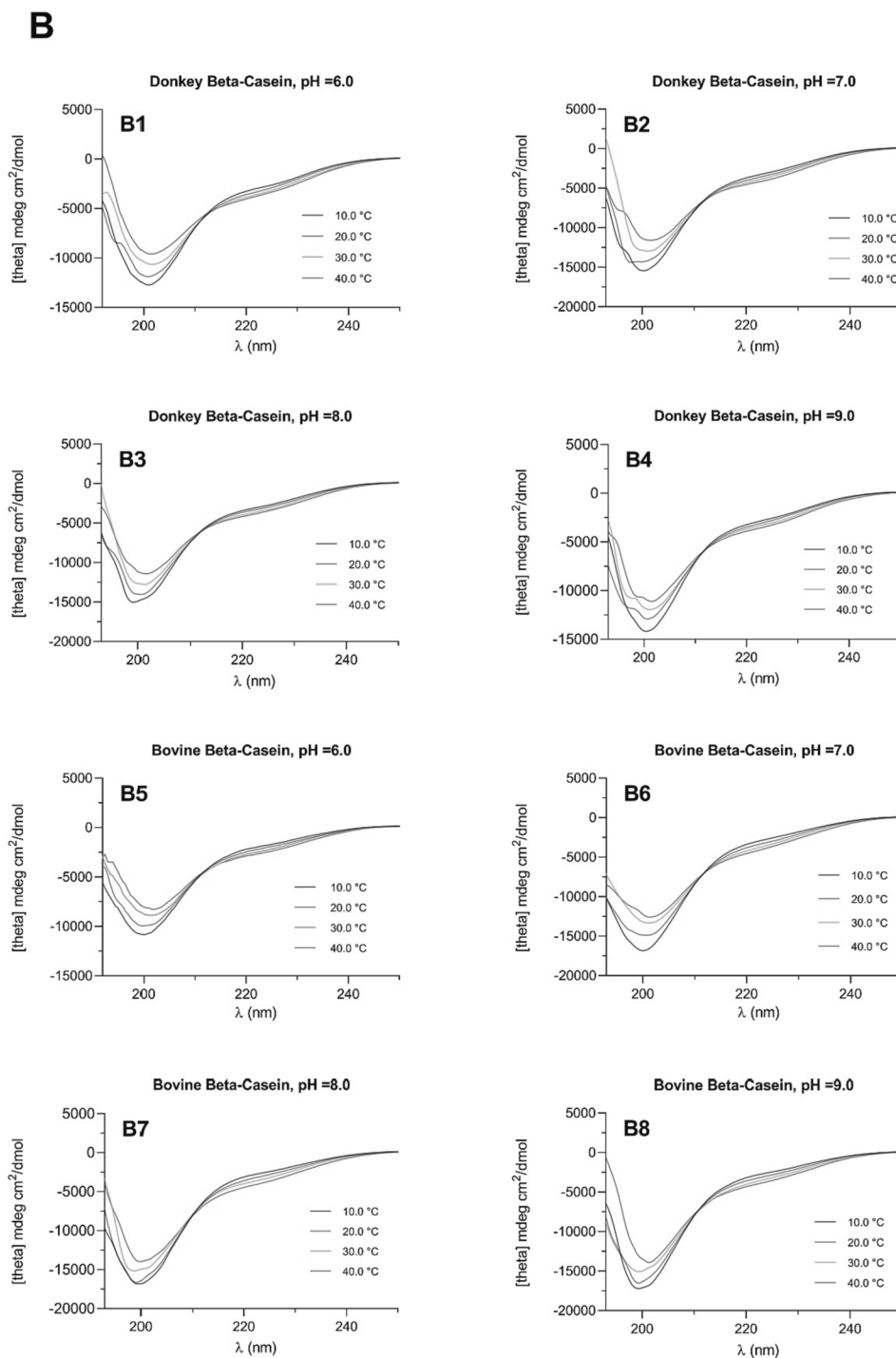


Fig. 4. (continued).

therefore favored by increasing protein concentration, increasing temperature and decreasing pH (as long as above the isoelectric point).  $\beta$ -CNs eventually populate a relaxed conformation at pH 9.0, less prone to micellization, in particular at low ionic strength (50 mM buffer).

Furthermore, the data obtained by Trp and ANS spectrofluorometric analysis of both donkey and bovine  $\beta$ -CNs have shown that the hydrophobic surface exposure properties were noticeably influenced by pH, temperature, and buffer concentration. In particular, a structural rearrangement leading to an increase in surface hydrophobicity of  $\beta$ -CNs has been mainly observed at the lower pH (pH 6.0), the higher temperature (50.0 °C), and at the higher buffer concentration (250 mM).

Based on these results it is possible to assess that pH, by modifying

the net charge of the protein, can strongly affect the propensity of both  $\beta$ -CNs to undergo the temperature-dependent transition involved in the micellization process. Both hydrophobic interactions and electrostatic repulsions are considered to play a role in the micellization of  $\beta$ -CN. The protonation of the acidic residues at a low pH can reduce the occurrence of charges of the phosphoserine residues in the N-terminal portion of the protein, thus minimizing electrostatic repulsion and favoring micellar self-assembly (Kumosinski et al., 1993; Lajnaf et al., 2021). The effect of pH was also observed on the enthalpy of micellization, which increased from pH 7 to pH 8 for both bovine and donkey  $\beta$ -CNs. In general, regardless the effect of pH, a remarkable difference in the self-assembly enthalpy between bovine and donkey  $\beta$ -CNs has emerged. This

difference in the thermodynamics of micellization can reflect a difference in the inter-molecular interactions involved in the micellar condensation: since hydrophobic contribution is mainly of entropic nature, the thermodynamic of micellization of donkey  $\beta$ -CN seems to be mainly driven by the hydrophobic tail rather than by electrostatic contribution, compared with the bovine protein.

Moreover, CD data have shown a temperature-induced increase in the degree of ordered structure at all pH values and in the range of temperature 10–40 °C, in which micellization occurs, as reflected by the slight increase in the ellipticity at 222 nm. Therefore, it can be assessed that under a pH-controlled favorable environment, the conditions for micellization upon heating are accompanied by an increase in the ordered secondary structure, predominantly represented by  $\alpha$ -helix and poly (Pro)II helix-like conformations. This behavior has been observed for both donkey and bovine  $\beta$ -CNs, and confirms the importance of the structural motifs organization of the C-terminal hydrophobic tail in the micellization process. Our results demonstrate that polyproline II helical structure favoring protein–protein interactions together with the promotion of a hydrophobic  $\alpha$ -helix in the C-terminal domain play a major role as structural determinants also for donkey  $\beta$ -CN self-association and micellization.

In conclusion, the temperature-induced, pH-dependent, hydrophobic surface exposure of both bovine and donkey's  $\beta$ -CNs, responsible for micelle formation, and observed by fluorescence spectroscopy, does collimate with the promotion of the  $\alpha$ -helical secondary structure of the hydrophobic C-terminal tail observed by CD spectroscopy. Together, these structural features are responsible for the CMC and CMT dependence on pH, temperature and ionic strength.

A biophysical characterization of the self-assembly of proteins is attracting more and more attention aimed at discovering new functions of liquid–liquid condensate states, by intrinsically disordered proteins (Fuxreiter & Vendruscolo, 2021). The results of this work can provide structural information and insight on critical parameters promoting intra and inter-molecular interactions involved in micellization for the development of  $\beta$ -CNs based nanocarriers useful to encapsulate bioactive compounds for pharmaceutical and nutraceutical applications.

#### CRedit authorship contribution statement

**Jingjing Zhang:** Conceptualization, Methodology, Formal analysis, Visualization, Investigation, Writing – original draft, Writing – review & editing. **Silvia Vincenzetti:** Investigation, Conceptualization, Supervision, Validation, Resources, Writing – review & editing. **Paolo Polidori:** Investigation, Conceptualization, Supervision, Validation, Resources, Writing – review & editing. **Valeria Polzonetti:** Visualization, Investigation, Supervision. **Alessandro Di Michele:** Visualization, Investigation, Conceptualization, Supervision, Validation, Resources, Writing – review & editing. **Guiqin Liu:** Visualization, Investigation, Supervision. **Lanjie Li:** Visualization, Investigation, Supervision. **Stefania Pucciarelli:** Investigation, Conceptualization, Supervision, Validation, Resources, Writing – review & editing.

#### Declaration of Competing Interest

The authors declare that they have no known competing financial interests or personal relationships that could have appeared to influence the work reported in this paper.

#### Data availability

Data will be made available on request.

#### Acknowledgments

The authors would like to thank Mrs Natalina Cammertoni for her

excellent technical support.

#### Appendix A. Supplementary material

Supplementary data to this article can be found online at <https://doi.org/10.1016/j.foodchem.2023.137285>.

#### References

- Annan, W. S., Fairhead, M., Pereira, P., & Walle, C. F.v.d. (2006). Emulsifying performance of modular  $\beta$ -sandwich proteins: The hydrophobic moment and conformational stability. *Protein Engineering, Design and Selection*, 19(12), 537–545. <https://doi.org/10.1093/protein/gz041>
- Anema, S. G. (2021). Heat-induced changes in caseins and casein micelles, including interactions with denatured whey proteins. *International Dairy Journal*, 122(105136). <https://doi.org/10.1016/j.idairyj.2021.105136>
- Bradford, M. M. (1976). A rapid and sensitive method for the quantitation of microgram quantities of protein utilizing the principle of protein-dye binding. *Analytical Biochemistry*, 72(1–2), 248–254. [https://doi.org/10.1016/0003-2697\(76\)90527-3](https://doi.org/10.1016/0003-2697(76)90527-3)
- Boulet, M., Britten, M., & Lamarche, F. (2001). Dispersion of food proteins in water-alcohol mixed dispersants. *Food Chemistry*, 74(1), 69–74. [https://doi.org/10.1016/S0308-8146\(01\)00099-1](https://doi.org/10.1016/S0308-8146(01)00099-1)
- Chakraborty, A., & Basak, S. (2008). Effect of surfactants on casein structure: A spectroscopic study. *Colloids and Surfaces B: Biointerfaces*, 263, 83–90. <https://doi.org/10.1016/j.colsurfb.2007.11.005>
- Chia, J., McRae, J., Kukuljan, S., Woodford, K., Elliott, R., Swinburn, B., & Dwyer, K. (2017). A1 beta-casein milk protein and other environmental pre-disposing factors for type 1 diabetes. *Nutrition & Diabetes*, 7(5), e274–e. <https://doi.org/10.1038/nutd.2017.16>
- Chianese, L., Calabrese, M. G., Ferranti, P., Mauriello, R., Garro, G., De Simone, C., & Ramunno, L. (2010). Proteomic characterization of donkey milk “caseome”. *Journal of Chromatography A*, 1217, 4834–4840. <https://doi.org/10.1016/j.chroma.2010.05.017>
- Dauphas, S., Mouhous-Riou, N., Metro, B., Mackie, A., Wilde, P. J., Anton, M., & Riaublanc, A. (2005). The supramolecular organisation of  $\beta$ -casein: Effect on interfacial properties. *Food Hydrocolloids*, 19(3), 387–393. <https://doi.org/10.1016/j.foodhyd.2004.10.005>
- Ellouze, M., Vial, C., Attia, H., & Ayadi, M. A. (2021). Effect of pH and heat treatment on structure, surface characteristics and emulsifying properties of purified camel  $\beta$ -casein. *Food Chemistry*, 365, Article 130421. <https://doi.org/10.1016/j.foodchem.2021.130421>
- Faizullin, D. A., Konnova, T. A., Haertlé, T., & Zuev, Y. F. (2017). Secondary structure and colloidal stability of beta-casein in microheterogeneous water-ethanol solutions. *Food Hydrocolloids*, 63, 349–355. <https://doi.org/10.1016/j.foodhyd.2016.09.011>
- Farrell, H. M., Wickham, E. D., Unruh, J. J., Qi, P. X., & Hoagland, P. D. (2001). Secondary structural studies of bovine caseins: Temperature dependence of  $\beta$ -casein structure as analyzed by circular dichroism and FTIR spectroscopy and correlation with micellization. *Food Hydrocolloids*, 15(4), 341–354. [https://doi.org/10.1016/S0268-005X\(01\)00080-7](https://doi.org/10.1016/S0268-005X(01)00080-7)
- Forrest, S. A., Yada, R. Y., & Rousseau, D. (2005). Interactions of vitamin D3 with bovine  $\beta$ -lactoglobulin A and  $\beta$ -casein. *Journal of agricultural and food chemistry*, 53(20), 8003–8009. <https://doi.org/10.1021/jf050661l>
- Fuxreiter, M., & Vendruscolo, M. (2021). Generic nature of the condensed states of proteins. *Nature cell biology*, 23(6), 587–594. <https://doi.org/10.1038/s41556-021-00697-8>
- Gangnard, S., Zuev, Y., Gaudin, J.-C., Fedotov, V., Choiset, Y., Axelos, M. A., Chobert, J.-M., & Haertlé, T. (2007). Modifications of the charges at the N-terminus of bovine  $\beta$ -casein: Consequences on its structure and its micellisation. *Food Hydrocolloids*, 21(2), 180–190. <https://doi.org/10.1016/j.foodhyd.2006.03.007>
- Hasni, L., Bourassa, P., Hamdani, S., Samson, G., Carpentier, R., & Tajmir-Riahi, H.-A. (2011). Interaction of milk  $\alpha$ - and  $\beta$ -caseins with tea polyphenols. *Food Chemistry*, 126(2), 630–639. <https://doi.org/10.1016/j.foodchem.2010.11.087>
- Helmick, H., Tonner, T., Hauersperger, D., Ettestad, S., Hartanto, C., Okos, M., ... Kokini, J. L. (2023). Physicochemical characterization of changes in pea protein as the result of cold extrusion. *Food Chemistry*, 423, Article 136240. <https://doi.org/10.1016/j.foodchem.2023.136240>
- Holt, C. (2013). Unfolded phosphopolypeptides enable soft and hard tissues to coexist in the same organism with relative ease. *Current opinion in structural biology*, 23(3), 420–425. <https://doi.org/10.1016/j.sbi.2013.02.010>
- Kuemin, M., Engel, J., & Wennemers, H. (2010). Temperature-induced transition between polyproline I and II helices: Quantitative fitting of hysteresis effects. *Journal of Peptide Science*, 16(10), 596–600. <https://doi.org/10.1002/psc.1245>
- Kumosinski, T., Brown, E., & Farrell, H., Jr (1993). Three-dimensional molecular modeling of bovine caseins: An energy-minimized  $\beta$ -casein structure. *Journal of dairy science*, 76(4), 931–945. [https://doi.org/10.3168/jds.S0022-0302\(93\)77420-2](https://doi.org/10.3168/jds.S0022-0302(93)77420-2)
- Laemmli, U. K. (1970). Cleavage of structural proteins during assembly of the head of bacteriophage T4. *Nature*, 227, 680–685.
- Lajnaf, R., Gharsallah, H., Attia, H., & Ayadi, M. A. (2021). Comparative study on antioxidant, antimicrobial, emulsifying and physico-chemical properties of purified bovine and camel  $\beta$ -casein. *LWT*, 140, Article 110842. <https://doi.org/10.1016/j.lwt.2020.110842>

- Li, M., Fokkink, R., Ni, Y., & Kleijn, J. M. (2019). Bovine beta-casein micelles as delivery systems for hydrophobic flavonoids. *Food Hydrocolloids*, 96, 653–662. <https://doi.org/10.1016/j.foodhyd.2019.06.005>.
- Licitra, R., Chessa, S., Salari, F., Gattolin, S., Bulgari, O., Altomonte, I., & Martini, M. (2019). Milk protein polymorphism in Amiata donkey. *Livestock Science*, 230, Article 103845. <https://doi.org/10.1016/j.livsci.2019.103845>
- Mendes, A. C., Baran, E. T., Reis, R. L., & Azevedo, H. S. (2013). Self-assembly in nature: Using the principles of nature to create complex nanobiomaterials. *WIREs Nanomed Nanobiotechnol.*, 5, 582–612. <https://doi.org/10.1002/wnan.1238>
- Mikheeva, L. M., Grinberg, N. V., Grinberg, V. Y., Khokhlov, A. R., & de Kruijff, C. G. (2003). Thermodynamics of micellization of bovine  $\beta$ -casein studied by high-sensitivity differential scanning calorimetry. *Langmuir*, 19(7), 2913–2921. <https://doi.org/10.1021/la026702e>.
- Moeiniafshari, A.-A., Zarrabi, A., & Bordbar, A.-K. (2015). Exploring the interaction of naringenin with bovine beta-casein nanoparticles using spectroscopy. *Food Hydrocolloids*, 51, 1–6. <https://doi.org/10.1016/j.foodhyd.2015.04.036>.
- Möller, M., & Denicola, A. (2002). Study of protein-ligand binding by fluorescence. *Biochemistry and Molecular Biology Education*, 30(5), 309–312. <https://doi.org/10.1002/bmb.2002.494030050089>.
- Monti, G., Bertino, E., Muratore, M. C., Coscia, A., Cresi, F., Silvestro, L., Fabris, C., Fortunato, D., Giuffrida, M. G., & Conti, A. (2007). Efficacy of donkey's milk in treating highly problematic cow's milk allergic children: An in vivo and in vitro study. *Pediatric Allergy and Immunology*, 18, 258–264. <https://doi.org/10.1111/j.1399-3038.2007.00521.x>
- O'Connell, J., Grinberg, V. Y., & De Kruijff, C. (2003). Association behavior of  $\beta$ -casein. *Journal of Colloid and Interface Science*, 258(1), 33–39. [https://doi.org/10.1016/S0021-9797\(02\)00066-8](https://doi.org/10.1016/S0021-9797(02)00066-8).
- Perinelli, D. R., Bonacucina, G., Cespi, M., Bonazza, F., Palmieri, G. F., Pucciarelli, S., Polzonetti, V., Attarian, L., Polidori, P., & Vincenzetti, S. (2019). A comparison among  $\beta$ -caseins purified from milk of different species: Self-assembling behaviour and immunogenicity potential. *Colloids and Surfaces B: Biointerfaces*, 173, 210–216.
- Portnaya, I., Cogan, U., Livney, Y. D., Ramon, O., Shimon, K., Rosenberg, M., & Danino, D. (2006). Micellization of bovine  $\beta$ -casein studied by isothermal titration microcalorimetry and cryogenic transmission electron microscopy. *Journal of Agricultural and Food Chemistry*, 54(15), 5555–5561. <https://doi.org/10.1021/jf060119c>.
- Qi, P. X., Wickham, E. D., & Farrell, H. M. (2004). Thermal and alkaline denaturation of bovine  $\beta$ -casein. *The Protein Journal*, 23(6), 389–402. <https://doi.org/10.1023/B:JOPC.0000039553.66233.3f>.
- Raak, N., Abbate, R. A., Lederer, A., Rohm, H., & Jaros, D. (2018). Size Separation Techniques for the Characterisation of Cross-Linked Casein: A Review of Methods and Their Applications. *Separations*, 5, 14. <https://doi.org/10.3390/separations5010014>
- Ranadheera, C., Liyanaarachchi, W., Chandrapala, J., Dissanayake, M., & Vasiljevic, T. (2016). Utilizing unique properties of caseins and the casein micelle for delivery of sensitive food ingredients and bioactives. *Trends in Food Science & Technology*, 57, 178–187. <https://doi.org/10.1016/j.tifs.2016.10.005>.
- Raynes, J., Day, L., Augustin, M. A., & Carver, J. (2015). Structural differences between bovine A1 and A2  $\beta$ -casein alter micelle self-assembly and influence molecular chaperone activity. *Journal of Dairy Science*, 98(4), 2172–2182. <https://doi.org/10.3168/jds.2014-8800>.
- Sharma, N., Sharma, R., Rajput, Y. S., Mann, B., Singh, R., & Gandhi, K. (2021). Separation methods for milk proteins on polyacrylamide gel electrophoresis: Critical analysis and options for better resolution. *International Dairy Journal*, 114, Article 104920. <https://doi.org/10.1016/j.idairyj.2020.104920>
- Schulte, J., Stöckermann, M., & Gebhardt, R. (2020). Influence of pH on the stability and structure of single casein microparticles. *Food Hydrocolloids*, 105, Article 105741. <https://doi.org/10.1016/j.foodhyd.2020.105741>.
- Shapira, A., Markman, G., Assaraf, Y. G., & Livney, Y. D. (2010).  $\beta$ -casein-based nanovehicles for oral delivery of chemotherapeutic drugs: Drug-protein interactions and mitoxantrone loading capacity. *Nanomedicine: Nanotechnology, Biology and Medicine*, 6(4), 547–555. <https://doi.org/10.1016/j.nano.2010.01.003>.
- Shevchenko, A., Tomas, H., Havli, J., Olsen, J. V., & Mann, M. (2006). In-gel digestion for mass spectrometric characterization of proteins and proteomes. *Nature protocols*, 1(6), 2856–2860. <https://doi.org/10.1038/nprot.2006.468>.
- Tidona, F., Criscione, A., Devold, T. G., Bordonaro, S., Marletta, D., & Vegarud, G. E. (2014). Protein composition and micelle size of donkey milk with different protein patterns: Effects on digestibility. *International Dairy Journal*, 35(1), 57–62. <https://doi.org/10.1016/j.idairyj.2013.10.018>
- Vincenzetti, S., Foghini, L., Pucciarelli, S., Polzonetti, V., Cammertoni, N., Beghelli, D., & Polidori, P. (2014). Hypoallergenic properties of donkey's milk: A preliminary study. *Veterinaria Italiana*, 50, 99–107. <https://doi.org/10.12834/VetIt.219.125.5>.
- Vincenzetti, S., Pucciarelli, S., Huang, Y., Ricciutelli, M., Lambertucci, C., Volpini, R., Scuppa, G., Soverchia, L., Ubaldi, M., & Polzonetti, V. (2019). Biomarkers mapping of neuropathic pain in a nerve chronic constriction injury mice model. *Biochimie*, 158, 172–179.
- Vincenzetti, S., Cammertoni, N., Rapaccetti, R., Santini, G., Klimanova, Y., Zhang, J.-J., & Polidori, P. (2022). Nutraceutical and Functional Properties of Camelids' Milk. *Beverages*, 8, 12. <https://doi.org/10.3390/beverages8010012>
- Whitmore, L., & Wallace, B. A. (2008). Protein secondary structure analyses from circular dichroism spectroscopy: Methods and reference databases. *Biopolymers: Original Research on Biomolecules*, 89(5), 392–400. <https://doi.org/10.1002/bip.20853>.
- Wu, K. Y., Yang, T. X., & Li, Q. Y. (2021). The effects of pH and NaCl concentration on the structure of  $\beta$ -casein from buffalo milk. *Food Science & Nutrition*, 9(5), 2436–2445. <https://doi.org/10.1002/fsn3.2157>
- Wüstneck, R., Fainerman, V. B., Aksenenko, E. V., Kotsmar, C., Pradines, V., Krägel, J., & Miller, R. (2012). Surface dilatational behavior of  $\beta$ -casein at the solution/air interface at different pH values. *Colloids and Surfaces A: Physicochemical and Engineering Aspects*, 404, 17–24. <https://doi.org/10.1016/j.colsurfa.2012.03.050>.
- Yousefi, R., Gaudin, J.-C., Chobert, J.-M., Pourpak, Z., Moin, M., Moosavi-Movahedi, A. A., & Haertle, T. (2009). Micellisation and immunoreactivities of dimeric  $\beta$ -caseins. *Biochimica et Biophysica Acta (BBA)-Proteins and Proteomics*, 1794(12), 1775–1783. <https://doi.org/10.1016/j.bbapap.2009.08.015>.
- Zhou, M., Xia, Y., Cao, F., Li, N., Hemar, Y., Tang, S., & Sun, Y. (2019). A theoretical and experimental investigation of the effect of sodium dodecyl sulfate on the structural and conformational properties of bovine  $\beta$ -casein. *Soft Matter*, 15, 1551–1561.
- Zhang, Z., Dalglish, D., & Goff, H. (2004). Effect of pH and ionic strength on competitive protein adsorption to air/water interfaces in aqueous foams made with mixed milk proteins. *Colloids and Surfaces B: Biointerfaces*, 34(2), 113–121. <https://doi.org/10.1016/j.colsurfb.2003.11.009>.